

Preliminary assessment of seismic site effects in the fluvio-lacustrine sediments of Kathmandu valley, Nepal

Dipendra Gautam^{1,2} · Deepak Chamlagain³

Received: 10 March 2015 / Accepted: 2 January 2016 / Published online: 13 January 2016
© Springer Science+Business Media Dordrecht 2016

Abstract Seismic site effects are predicted adopting ground response analysis for the fluvio-lacustrine deposits of Kathmandu Valley using available geotechnical data. Equivalent linearization of nonlinear soil model has been analyzed for the study area with the geotechnical database up to the engineering bedrock level. The amplification ratio has been estimated to be varying from 1.9 to 7.8. As the peak spectral acceleration and predominant period largely contribute in the damage of structures, higher values of these parameters are consistent with the damage during 1934 Bihar–Nepal earthquake. The peak spectral acceleration for Kathmandu Valley has been estimated in a close range of 1.2725–1.2826 g. Meanwhile, the predominant period of valley soil varies from 0.27 to 0.61 s, representing the possible resonance, as 3–6 stories structures are the majority constructions in the study area. It has been contemplated that the upper 30 m of Kathmandu Valley soil would undergo large amplification with higher spectral acceleration and the predominant period shows the higher possibility of resonance with the construction trend of the buildings. Past events have shown the severity of damage level during earthquake events in Kathmandu Valley; as the capital city with the highest population density is residing in this area, similar scenario of damage may be witnessed in future events as well, so incorporating the local site effects is must. Thus, the present study provides insights on the level of risk and possible geotechnical basis for the mitigation of inherited earthquake risk in the valley.

Keywords Nepal Himalaya · Kathmandu Valley · Seismic hazard · Seismic site effects · Amplification ratio

✉ Deepak Chamlagain
dchamlagain@hotmail.com

¹ Center for Postgraduate Studies, Nepal Engineering College, Pokhara University, Pokhara, Nepal

² Center for Disaster and Climate Change Studies, Kathmandu, Nepal

³ Department of Geology, Tri-Chandra Multiple Campus, Tribhuvan University, Ghantaghar, Kathmandu, Nepal

1 Introduction

Local subsurface geology, geomorphology, basin geometry and the geotechnical characteristics of the soil strata have a strong influence on seismic ground motion. After the 1906 San Francisco, USA, and 1923 Kanto earthquakes, Japan, it has been widely accepted that there is strong correlation with subsurface geology and earthquake damage. These seismic events have drawn attention of earthquake engineering profession on amplification characteristics of earthquake ground motion. Such characteristics, now widely known as seismic site effects, have been used to describe the influence of local geology on the ground motion and are widely recognized as an important factor of earthquake risk (e.g., Aki and Larner 1970; Aki 1993; Psarropoulos et al. 1999; Semblat et al. 2004; Psarropoulos et al. 2007; Lanzo et al. 2011; Chamlagain et al. 2013; Chamlagain and Gautam 2014). It has also become one of the major issues in the field of earthquake engineering because several observations made after the damaging earthquakes (e.g., Nigata and San Francisco, 1964; Irpinia, 1980; Mexico, 1985, Kobe, 1995, L'Aquila, 2009) revealed that the local amplification of earthquake ground motion has great influence on non-uniform damage pattern, particularly in soft fluvio-lacustrine deposit.

The Mexico earthquake of September 15, 1985, has clearly demonstrated the effects of soft soil on earthquake ground motion. The earthquake killed 9500 people about 30,000 were injured, more than 100,000 people were left homeless, and severe damage was caused in parts of Mexico City and in several states of central Mexico (Celebi et al. 1987). The peak ground acceleration at the epicentral area was about 0.14 g. The maximum accelerations were about 0.04 g at the rock sites of the city area some 400 km away from the epicenter. The maximum acceleration reached to 0.17 g at the soft clay deposit of the city. The amplification ratio of earthquake ground motion was the main culprit for the observed damages (Celebi et al. 1987). Having the similar geological condition and location in the active collision plate boundary of the Indian and Eurasian plates, Kathmandu Valley witnessed a massive damage during the 1934 Bihar–Nepal earthquake. Although the epicenter of 8.1 M_w earthquake was located some 250 km northeast of Kathmandu Valley, about 4296 people were killed, destroyed about 19 % and damaged about 38 % of the valley buildings (Pandey and Molnar 1988; Rana 1935). The observed damage was mainly observed in the area having thick clay deposits mainly in the southeastern part of the valley. The level of destruction particularly in Bhaktapur City in the eastern part of the valley and neighboring areas was found to be the highest (Pandey and Molnar 1988; Rana 1935). Besides these, many historical temples and monuments also collapsed or sustained severe damage. As per the present-day urbanization pattern, Japan International Cooperation Agency (JICA 2002) estimated a total of 59,000 houses would be destroyed, 18,000 deaths and 59,000 seriously injured if the earthquake having equal magnitude of 1934 Bihar–Nepal hits the Kathmandu Valley. Similarity of geology and geotechnical properties as that of Mexico City has drawn the attention in estimating the effect of local geology during earthquake events for a deep alluvial valley. Thus, in this contribution, considering the observed damage pattern of 1934 Bihar–Nepal earthquake and probability of occurrence of similar nature and magnitude of earthquake in the central seismic gap, we aim to assess seismic site effects of the soft fluvio-lacustrine deposits of the Kathmandu Valley.

2 Kathmandu Valley

Kathmandu Valley is located in the central part of Nepal and comprised of three districts, namely Kathmandu, Bhaktapur and Lalitpur (Fig. 1). The major administrative centers and capital city, Kathmandu, are located in the valley. There are five municipalities, namely Kathmandu Metropolitan City (KMC), Lalitpur Sub-Metropolitan City (LSMC), Bhaktapur Municipality, Madhyapur Municipalities and Kirtipur Municipalities. Recently, Government of Nepal has upgraded remaining semi-urban areas in various municipalities declaring entire valley as the urban areas. The KMC is the largest municipality and consists of most of the central government offices. Besides these, the Kathmandu Valley hosts most of the world heritage site of Nepal.

This study is mainly focused on KMC and LSMC, where about 1.23 million people reside within an area of 64.6 km², and thus, the population density is estimated to be 19,040/km² (CBS 2011). The trend of the urbanization in the Kathmandu Valley is rapidly changing. KMC and LSMC with haphazard mushrooming trend of building construction

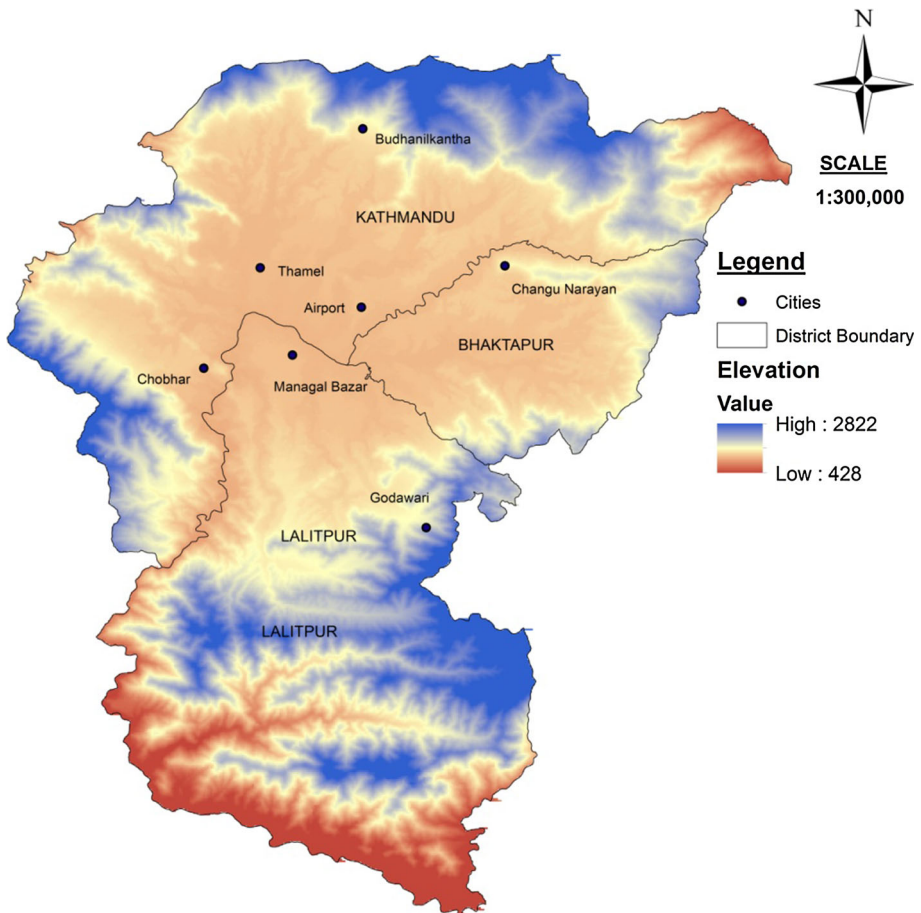


Fig. 1 Digital elevation model of Kathmandu Valley

have accommodated 309,512 houses. The inception of modern reinforced construction (RC) started around four decades back; subsequently, it has also downsized other construction practices in Kathmandu Valley; however, still around 20 % of buildings are mud mortar-bonded brick/stone unreinforced masonry construction, about 35 % of buildings are cement-bonded unreinforced masonry construction, and nearly 45 % of buildings are RC construction (CBS 2011). Being the location of capital city, Kathmandu Valley has been growing rapidly without considering required disaster management measures. The severity of the risk has been more than the 1934 Bihar–Nepal earthquake, as the valley population has already risen by more than sevenfold and there is no significant improvement in building construction practices (Bhattarai and Conway 2010).

3 Geotectonic setting

3.1 Brief geology of Nepal Himalaya

Himalaya was formed by the continuous subduction followed by collision between the Indian and Eurasian plate for 50 million years (Patriat and Achache 1984; Rowley 1996) at the rate of 35–38 mm/year toward N–NE (Chen et al. 2000; Holt et al. 2000; Paul et al. 2001; Wang et al. 2001; Sella et al. 2002; Jouanne et al. 2004) and is regarded to be seismically one of the active zones in the world. The convergence is highlighted through shortening across the Himalaya, Tibetan Plateau and Tien Shan, and by Tibetan deformation through eastward movement of crustal material and southern rotation about the eastern syntaxis (Molnar and Lyon-Caen 1989; Wang et al. 2001; Zhang et al. 2004; Chamlagain and Hayashi 2007).

Similar to the entire Himalayan belt, Nepal Himalaya consists of the five tectonic zones running east to west (Fig. 2a, b): (1) The Terai tectonic zone dominated by the recent alluvial deposition over 1 km thick concealing the Churia Group (Sivalik equivalents) and underlying rocks of northern peninsular India, (2) the Churia Zone with the Neogene to Quaternary foreland basin deposition, regarded to be the active part of Himalaya, (3) the Lesser Himalaya, with sedimentary rocks deposited on the Indian continental margin, (4) Higher Himalaya, consisting of crystalline high grade metamorphic rocks and (5) Tibetan–Tethys zone, with Cambrian to Cretaceous–Eocene fossiliferous sedimentary rocks overlying the crystalline rocks of Higher Himalaya (Upreti 1999).

The architecture of Nepal Himalaya is governed by three master thrusts (Fig. 2a) extending along east–west throughout the Himalayan range: the Main Central Thrust (MCT), the Main Boundary Thrust (MBT) and the Main Frontal Thrust (MFT) (Fig. 2b). However, the master thrusts, along with the South Tibetan Detachment Fault System (STDFS), converge to form a low-angle decollement (plate boundary mega-thrust), the Main Himalayan Thrust (MHT), which runs along north–south. The geophysical and seismological studies conducted till date have shown that the MHT and other associated faults are responsible for ongoing seismicity in the region (Seeber and Armbruster 1981; Baranowski et al. 1984; Pandey et al. 1995, 1999). The mid-crustal ramp situated beneath the Higher Himalaya is acting like a geometrical asperity, where high accumulation of elastic stress and strain during inter-seismic periods. The accumulation of shear stress in the ramp and two flat sides of the MHT may lead to reactivation of the Himalayan geological structures by major earthquakes ($M_w > 8$) in the coming days (Chamlagain and Hayashi 2007).

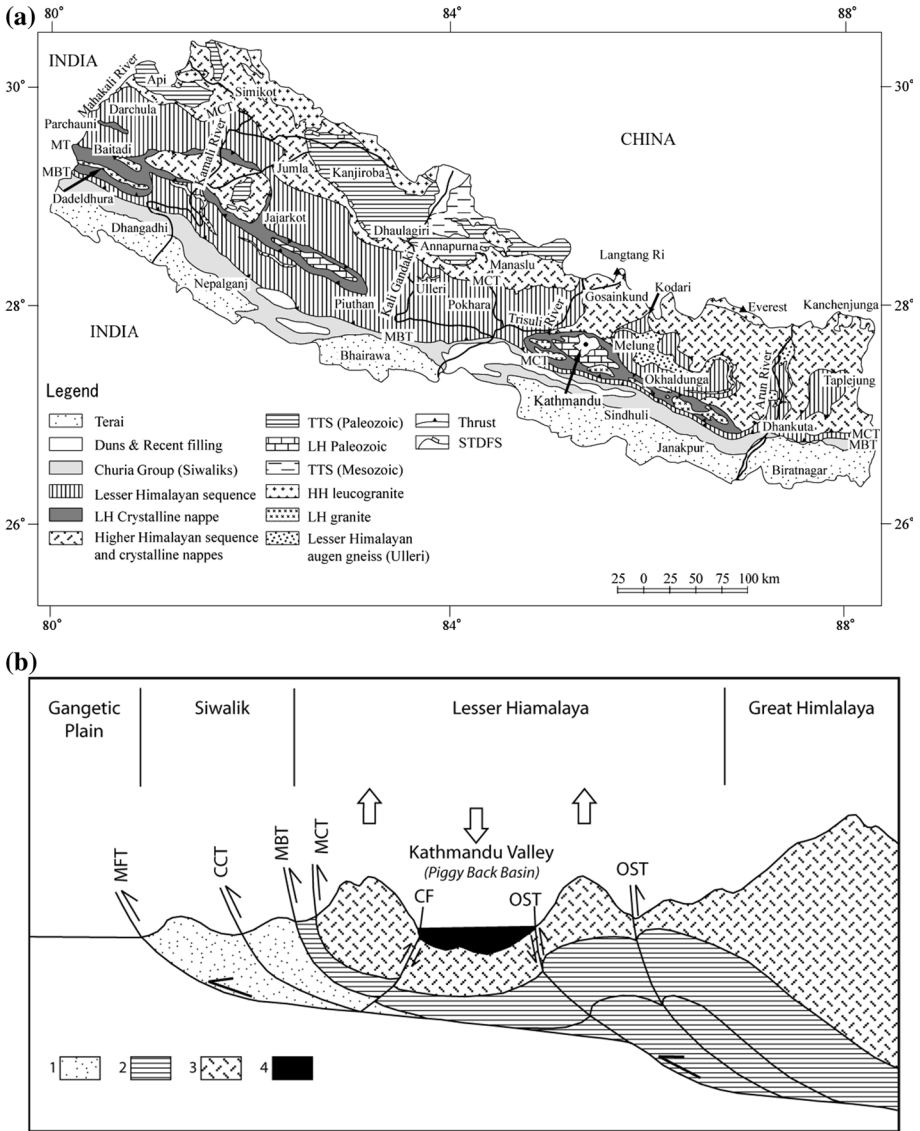


Fig. 2 **a** Geological map of Nepal (modified after Upreti and Le Fort 1999). *LH* Lesser Himalaya, *HH* Higher Himalaya, *TTS* Tibetan-Tethys sequence, *MBT* Main Boundary Thrust, *MCT* Main Central Thrust, *MFT* Main Frontal Thrust, *STDS* South Tibetan Detachment System. **b** Simplified geological cross section across central Nepal. *CCT* Central Churia Thrust, *OST* out-of-sequence thrust (Sakai 2001a). 1 Siwalik, 2 Lesser Himalaya, 3 Higher Himalaya, 4 Kathmandu Basin

3.2 Geology of Kathmandu Valley

Kathmandu Valley is an intermontane basin with young fluvio-lacustrine sediment deposit of Pliocene to Quaternary age in the Lesser Himalaya zone of Nepal. It has thick sediment deposit up to 500 m (Yoshida and Igarashi 1984; Dill et al. 2001, 2003) with huge

occurrence of fluvio-lacustrine unconsolidated sediments in the central part and outcropping bedrock in the peripheral region. Distribution of sediments is non-uniform in Kathmandu Valley (Fig. 3a), as the central part is characterized by larger thickness of sediments than the peripheral part. The central part of the valley consists of Bagmati Formation, Kalimati Formation and Patan Formation; among these, the Bagmati Formation was active before the lake formation in valley and is taken to be responsible for deposition of sediments in most part of the valley (Fig. 3b). Kalimati Formation is the black clayey deposit abundantly occurring in the central part with dark gray carbonaceous beds of the open lacustrine facies. The Patan Formation is distributed in and around KMC and LSMC, consisting of fine to medium sand and silt interbedded with clay and fine gravels in some places. Northern and northeastern part of Kathmandu Valley consists of fluvio-deltaic or fluvio-lacustrine origin primarily sandy facies known as Gokarna Formation and Thimi Formation (Yoshida and Igarashi 1984; Sakai 2001a, b, c). Tarebhir Fault and Chandragiri Fault in the southern part of Kathmandu Valley are considered to be active faults, which are intersecting the colluvial slopes and the terraces of the late Pleistocene age (Sakai 2001a, b, c). The basement rock in the Kathmandu Valley consists of Phulchoki Group and Bhimpheedi Group of the Kathmandu Complex (Stocklin and Bhattarai 1977).

4 Seismicity in Nepal Himalaya

The Himalayan arc has witnessed many major earthquakes (e.g., 1897 Shillong earthquake, $M_w = 8.1$; 1905 Kangra earthquake, $M_w = 7.8$; 1934 Bihar–Nepal earthquake, $M_w = 8.1$; 1950 Assam earthquake $M_w = 8.7$; 1988 Udaypur earthquake $M_w = 6.5$; 1991 Uttarkashi earthquake, $M_w = 6.9$; 2005 Kashmir earthquake, $M_w = 6.2$, and $M_w = 6.9$; and 2011 Sikkim–Nepal boarder earthquake) with rupture lengths of several hundred kilometers (Bilham 1995; Seeber and Armbruster 1981; USGS 2011). Recently, on April 25, 2015, $M_w = 7.8$ Gorkha earthquake occurred some 80 km northwest of the Kathmandu Valley unzipping the lower edge of the locked portion of the MHT that ruptures about 140-km-long segment toward east of the epicenter (Avouac et al. 2015; Galetzka et al. 2015). The Gorkha earthquake is an example of large continental mega-thrust because rupture propagated eastward radiating high-frequency seismic waves as the slip pulses propagated along the locked zone with high and heterogeneous pre-seismic stress, which was resumed during the aftershock of $M_w = 7.3$ on May, 12, 2015 (Avouac et al. 2015).

While considering the events after 1800 AD, the estimated minimum slip deficit for around 60 % of the arc is 4 m, which may lead to several major earthquakes in this region, with possibility of 10-m slip while depending on reliability of the historic record prior to these events (Bilham et al. 2001). At this juncture, it is believed that the central seismic gap (area between Dehra Dun and Kathmandu) of the western Nepal has not been ruptured since 1505 and indicates 9 m of accumulated potential slip, with assumption that the fault is fully locked, which might cause a major earthquake $M_w > 8$ (Bilham and Ambraseys 2004). It is believed that the 2015 Gorkha earthquake did not release the total accumulated energy in the western Nepal (Avouac et al. 2015).

The distribution of microseismicity in Nepal has revealed three distinct clusters (Pandey et al. 1999). In western Nepal, it lies between 80.5°E and 82.5°E; in central Nepal, it lies between 82.5°E and 86.5°E, and the eastern Nepal cluster is located in between 86.5°E and 88.5°E. The general trend has been depicted to be of narrow belt of predominantly moderate-sized earthquakes below the Lesser Himalaya and just south of the Higher

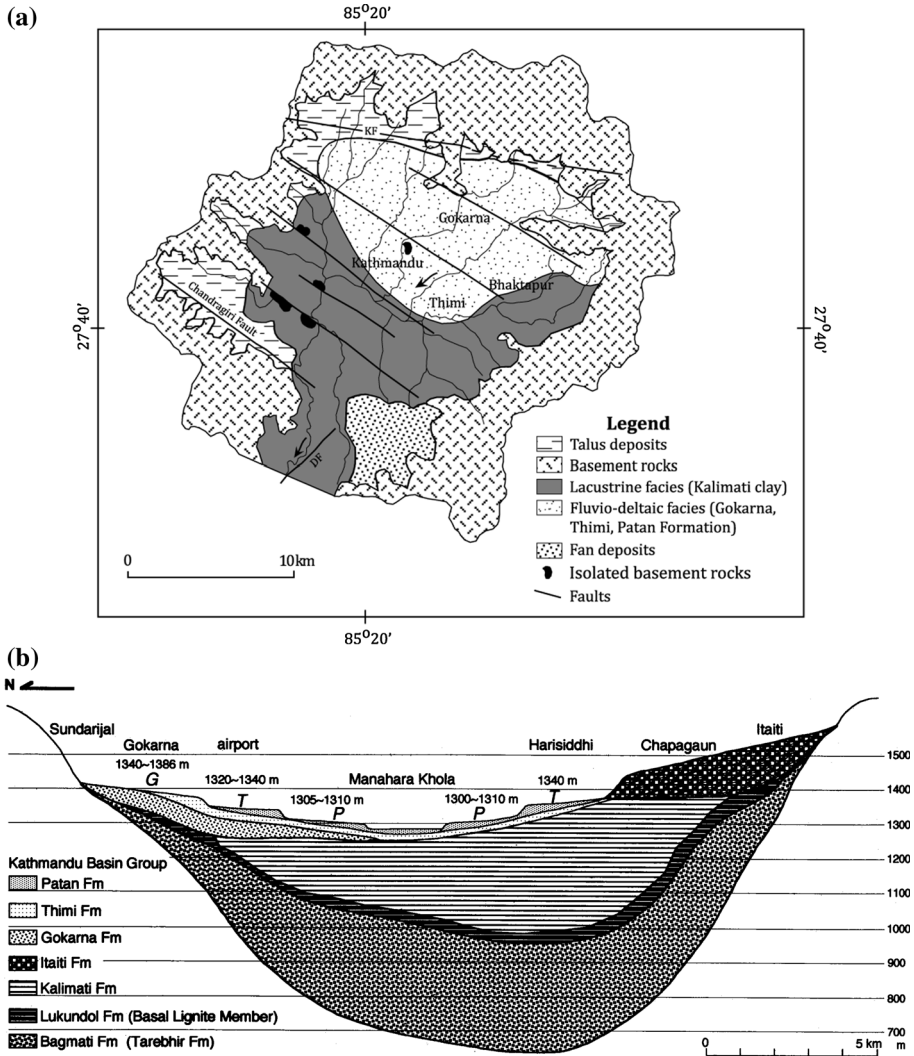


Fig. 3 **a** Geological map of Kathmandu Valley (Sakai 2001b). **b** North-south schematic section of the Kathmandu Valley (Sakai 2001c)

Himalayan front (Ni and Barazangi 1984); moreover, the great Himalayan earthquakes have followed the trend of occurring along the basal decollement beneath the Siwalik and the Lesser Himalaya with their focal depth varied between 10 and 20 km (Fig. 4). The mid-crustal ramp model illustrates the mechanism of earthquake generation in the Himalaya; stating that during the inter-seismic period due to the locking of southern ramp-flat segment of MHT, strain is being accumulated, whenever it exceeds the threshold, the stress releasing would lead to the great earthquakes along the MHT (Pandey et al. 1999) although it doesn't address the mantle earthquakes like the Udaypur earthquake that caused extensive damage in eastern Nepal. Similarly, Kathmandu Valley has severely been hit by the earthquakes of magnitude greater than M_w 8.0 within a few hundred years period

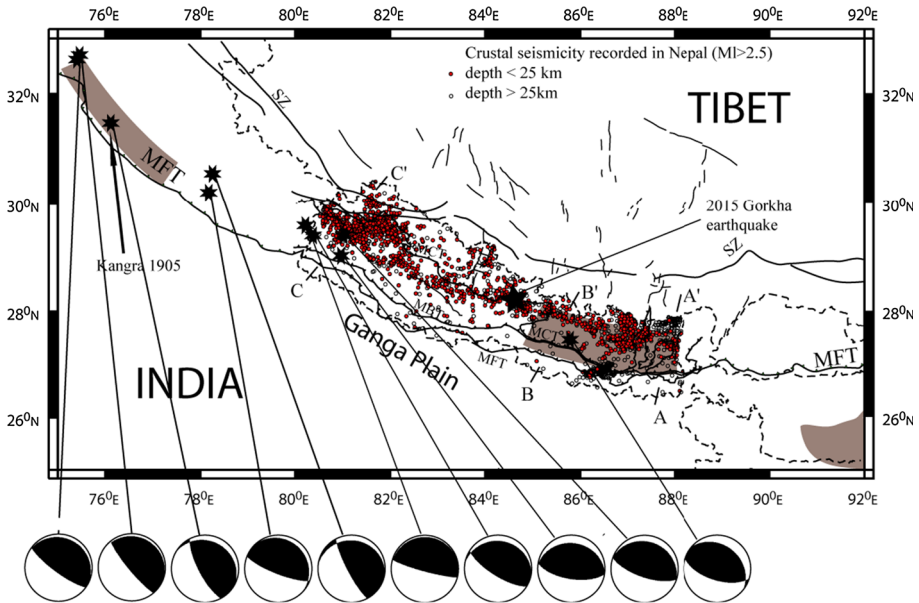


Fig. 4 Seismicity in the Himalayas of Nepal (modified after Jouanne et al. 2004); the intense microseismicity (monitored between 1985 and 1998) drawn with *small gray circles*, tend to cluster south of the Higher Himalayas (Pandey et al. 1999) at a mid-crustal level. Stars representing medium-size earthquake

(Seeber et al. 1981; Molnar 1984). The major events taken place in 1255, 1408, 1681, 1803, 1810, 1833 and 1866 have devastated Kathmandu Valley (Chitrakar and Pandey 1986; Gupta 1988; Bilham et al. 1995; Pandey et al. 1995). Thus, the valley is considered as one of the high-risk areas because of its location, soft and fragile geological formation and ongoing non-engineered construction practices.

5 Geotechnical characterization

Kathmandu Valley is filled by fluvio-lacustrine soft sediment deposit with highly variation in thickness. Moribayashi and Maruo (1980) estimated that the thickness of Kathmandu Valley soft soil deposit is to be 650 m through gravity measurements; in addition to this, a muddy and sandy sequence of more than 300 m thick has been observed in Kathmandu Valley (Katel et al. 1996) from drilling data at various sites. An organic black cotton soil is widely distributed in the Kathmandu Valley, and the major proportion is found in the central part of the valley.

Analysis of 49 borehole logs reaching a maximum depth of 30 m has been performed. As a crude approximation, to investigate the site response of the upper valley deposit, the engineering bedrock ($V_s = 700$ m/s) was placed at 30 m in all boreholes to model an elastic base.

The studied boreholes suggest that the uppermost layer ranging up to depth of 1.5 m is covered by either top soil or filling materials; mushroomed construction in last two decades has overshadowed the top soil covering of the Kathmandu Valley. Immediately below such

layer, the dark gray sandy silt is dominant in most of the study sites. This layer is followed by low plasticity silt and then medium plasticity silt; the subsequent layer is usually of stiff clay with low-to-medium plasticity. As per the geotechnical characterization of Kathmandu Valley, it has been inferred that the low-to-medium plasticity silt to clay is dominant throughout the valley and the groundwater table is variously reported to be found to upper to lower depths as well.

In the absence of geophysical tests, the shear wave velocity was estimated through the correlation with corrected SPT values proposed by JICA for the alluvial deposit of the Kathmandu Valley: $V_s = 97 N^{1/3}$ for all types of soils. According to this correlation, V_s varies from 148 to 297 m/s in the valley. Representative borehole logs with the shear wave profile are presented in Fig. 5. It has been found that the entire region of KMC and LSMC abundantly constitutes clay with the plasticity index variation of 0–15, and moreover, the medium clay silt has been found to be constituted with the plasticity index of 23. As there is no experimental evaluation of nonlinear dynamic soil properties for the fluvio-lacustrine deposit, normalized shear modulus and damping ratio curves proposed by Vucetic–Dobry (1991) for different values of plasticity index have been adopted for this study (Fig. 6).

6 Seismic site effects analysis

Broadly, seismic site effects are the modifications in intensity, duration and frequency content of the incoming wave motion due to the local geology and the topographic features. It has significant effects on the structural response during earthquakes, and thus, the damage is dependent over the site condition. Generally, thicker layers of soft, unconsolidated deposits tend to amplify selectively at different wave frequencies.

6.1 Methodology: equivalent linear site response analysis

Modeling site effects with true nonlinear constitutive models needs an accurate identification of dynamic soil properties; however, such information are not easily available, and equivalent linearization of nonlinear behavior is widely preferred in most of the ground response analyses. Therefore, in order to estimate the one-dimensional site effects, the equivalent linear site response approach has been implemented in this study. For seismic site effects analysis purpose, Equivalent Linear Earthquake Site Response Analysis (EERA) is used. It was developed in FORTRAN 90 in 1998 with the same basic concept as that of well-known SHAKE code; moreover, EERA is the modern implementation of established concepts of equivalent linear earthquake site response analysis and its advantage hinges with the dynamic array dimensioning and matrix operations in FORTRAN 90 (Bardet et al. 2000). With the facility of allocating strata as much as needed, EERA is used for assessing the ground response analysis due to its user friendliness and convenience over calculations overcoming the limitations of SHAKE 91, and the use of dynamic library in FORTRAN 90. The size of arrays adapts to the size of the problems within the limit of the available memory of computer. EERA dimensions internally its work arrays depending on the problem size; however, total number of sub-layers and material properties are limited to 50 and 13, respectively, in case of SHAKE 91, but in the other hand, there is no limitation on sub-layering and material property input in EERA. The number of data points for fast Fourier transform (FFT) could be prescribed behind 4096, and thus, time series recording of as many as available could be deployed as the inputs in

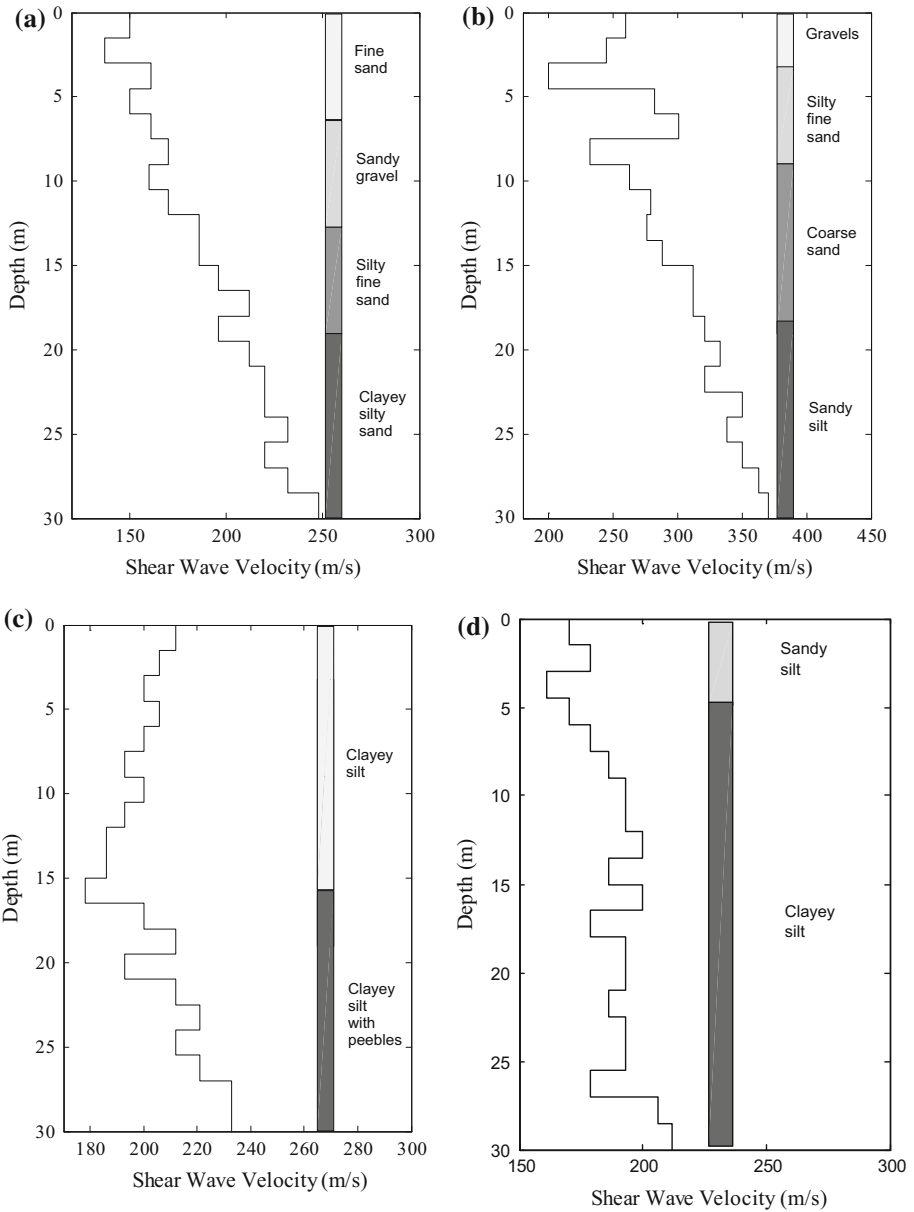


Fig. 5 Borehole log with shear wave velocity profile at **a** Hattiban, **b** Dhapasi, **c** Nakhu, **d** Balkumari

EERA, leading to better modeling of strong ground motion and subsequent acquaintance with the ground response as well. The significances of EERA over the other codes are the relative velocity and displacement at each sub-layer could be calculated like the acceleration, and the users could select filtered as well as unfiltered object motion.

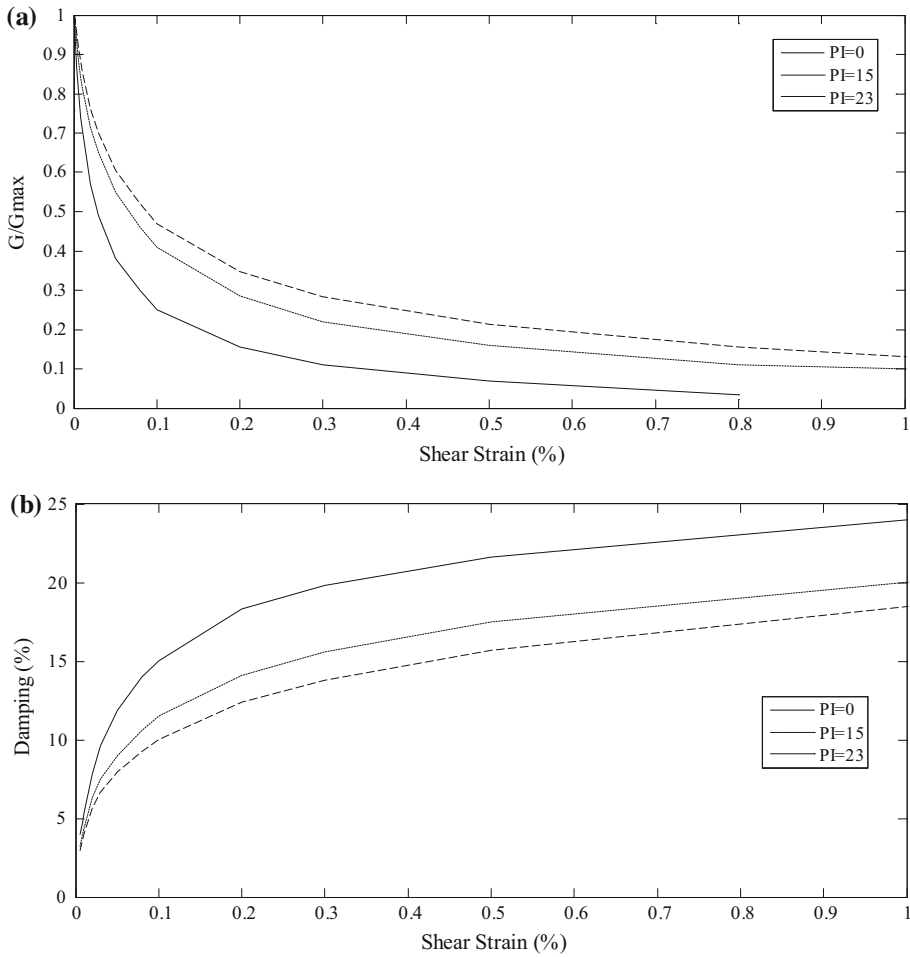


Fig. 6 Nonlinear material properties: variation of **a** normalized shear modulus- G/G_{max} and **b** damping ratio with shear strain amplitude (after Vucetic–Dobry 1991)

6.2 Input motion

For the site effect analysis, the Uttarkashi earthquake ($M_w = 6.9$) of October 20, 1991, has been used as the input motion. Acceleration time history was recorded on bedrock of Uttarkashi station at 34 km of epicentral distance. The Uttarkashi earthquake is chosen to be the input motion due to fact that the nature, type and tectonic setting of the earthquake are similar to the earthquake patterns in Nepal Himalaya. Modeling KMC and LSMC could be more reliable through this time history as the possible sources (MBT and MFT) of earthquakes in Kathmandu Valley are within the comparable radii of Uttarkashi epicenter. No scaling was therefore applied to the recordings. The double cycle acceleration time history shows the peak value of 0.32 g at 5.86 s (Fig. 7), the peak velocity recorded is 18.35 cm/s at 5.80 s (Fig. 8), and the corresponding peak spectral acceleration is 1.3 g at 0.29 s (Fig. 9).

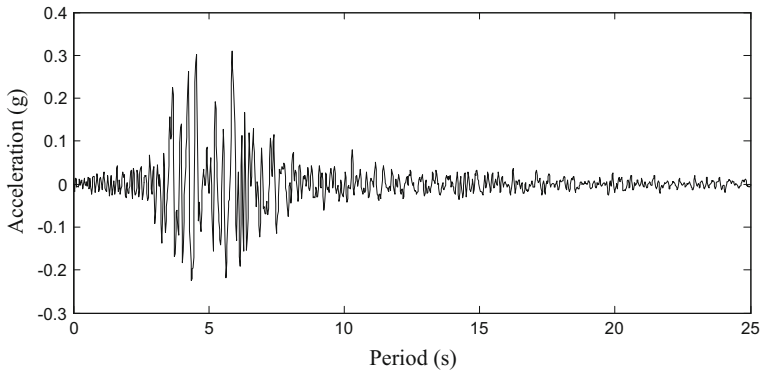


Fig. 7 Acceleration time history of the Uttarkashi earthquake

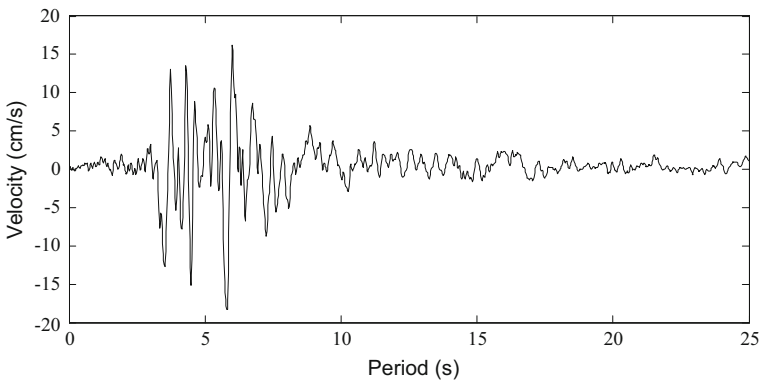


Fig. 8 Velocity time history for the Uttarkashi earthquake

7 Results

Altogether 49 spatially distributed borehole logs are simulated using one-dimensional EERA code. The results are presented in the form of distribution maps for amplification ratio, spectral acceleration and predominant period.

7.1 Amplification ratio

The amplification ratios of spectral values vary greatly with seismic intensity; lower shaking intensity earthquakes introduce higher amplification ratios due to more linear elastic soil behavior, contrary to higher intensities where soils are exhibiting nonlinear behavior resulting from decrease in peak spectral values. In this study, higher amplification ratio has been observed around Thamel, Maharajgunj, Chabhill, Boudha, Sundhara, Kalimati and Khumaltar. These areas are characterized dominantly clay, silty clay and fine sand and silt deposits. The amplification spectrum for the few representative areas is shown in Fig. 10. For the Balkumari area, maximum amplification ratio is obtained as 3.782 at the frequency of 1.0 Hz (Fig. 10a); similarly, for Maharajgunj, the value of maximum

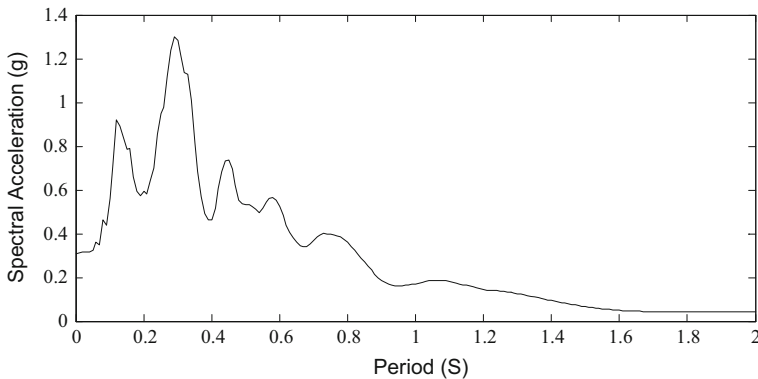


Fig. 9 Response spectra for the Uttarkashi earthquake

amplification ratio is obtained as 6.87 at the frequency of 2.60 Hz (Fig. 10b). Likewise, in Hariharbhawan, the value of maximum amplification ratio is estimated as 3.40 at the frequency of 1.60 Hz (Fig. 10c). Similarly, for Sinamangal area (nearby Tribhuvan International airport) amplification value 5.10 is obtained at the frequency of 3.40 Hz (Fig. 10d). For core city of Thamel area, the maximum amplification is estimated to be 7.78 at the frequency of 2.60 Hz (Fig. 10e), and for the New Road, it is estimated to be 5.53 at the frequency of 2.80 Hz (Fig. 10f). The dominant frequency of peak amplification in the fluvio-lacustrine deposit is found to be varied in between 1 and 3.6 Hz. Overall, the amplification ratio in the study area has been found to be varying between 1.85 and 7.89 (Fig. 11). The study has clearly shown that the fluvio-lacustrine sediments comprising dominantly of clay and silty clay (for detail, see Sakai 2001a, b, c) amplify greatly during the earthquake excitation. The average shear wave velocity for the upper 30 m ($V_{s,30}$) is one of the key parameters that governs the amplification ratio. The $V_{s,30}$ values varies from 148 to 298 m/s in the study areas (Fig. 12). Lower values are mostly found in the clay to silty clay-dominated western to southern part of the valley, i.e., adjoining areas of Thamel, Kalimati, Sundhara, Airport area, Jawalakhel and Khumaltar, where the amplification ratio is relatively higher. In contrast, the northeastern part (Chabhil) shows higher value of $V_{s,30}$ and lower amplification.

7.2 Spectral acceleration

The current urban construction practices in Kathmandu Valley have revealed the dominance of three-, four- and five-storied reinforced concrete residential buildings, and most of these are constructed as owner built houses. Therefore, spectral accelerations computed at 0.3, 0.4 and 0.5 s are quite significant to estimate vulnerability of the buildings and spectral acceleration maps are, thus, presented accordingly.

The spectral accelerations at 0.3 s is relatively higher, spanning in a range of 1.25–1.32 g (Fig. 13). The higher value is mainly found in the northern part of Thamel and is about 1.32 g. The NE–SW striking area from Boudha to Nakhu distinctly shows the spectral acceleration ranging from 1.28 to 1.29 g; remaining areas show lower value. In the same way, at the time period of 0.4 s, the range of spectral acceleration in the study area varies between 0.46 and 0.46 g (Fig. 14), a one-third of the acceleration at 0.3 s with

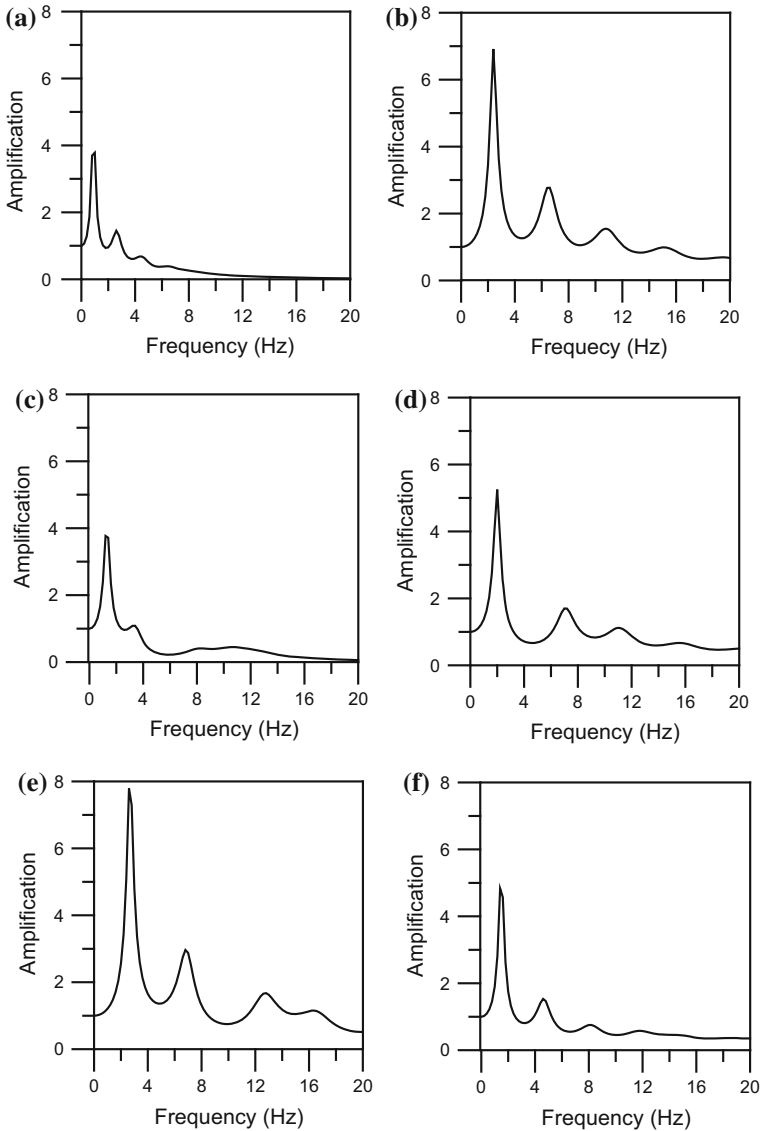


Fig. 10 Representative equivalent linear amplification factors at **a** Balkumari, **b** Maharajgunj, **c** Hariharbhawan, **d** Sinamangal, **e** Thamel, **f** New road

almost similar pattern. Interestingly, the spectral acceleration has shown almost similar pattern, but bit higher values, in the range of 0.53–0.54 g at 0.5 s (Fig. 15).

The peak spectral acceleration lies in the range of 1.27–1.28 g (Fig. 16) a very close but high range. The maximum peak spectral acceleration (1.28 g) has been obtained in and around Thamel, Sundhara, Boudha, Naya Baneshwor, Jawalakhel and Nakkhu. The core area of Thamel has computed a maximum peak spectral acceleration, i.e., 1.28 g at 0.32 s (Figs. 16, 17). In this area, as per the geotechnical model, the boreholes are characterized

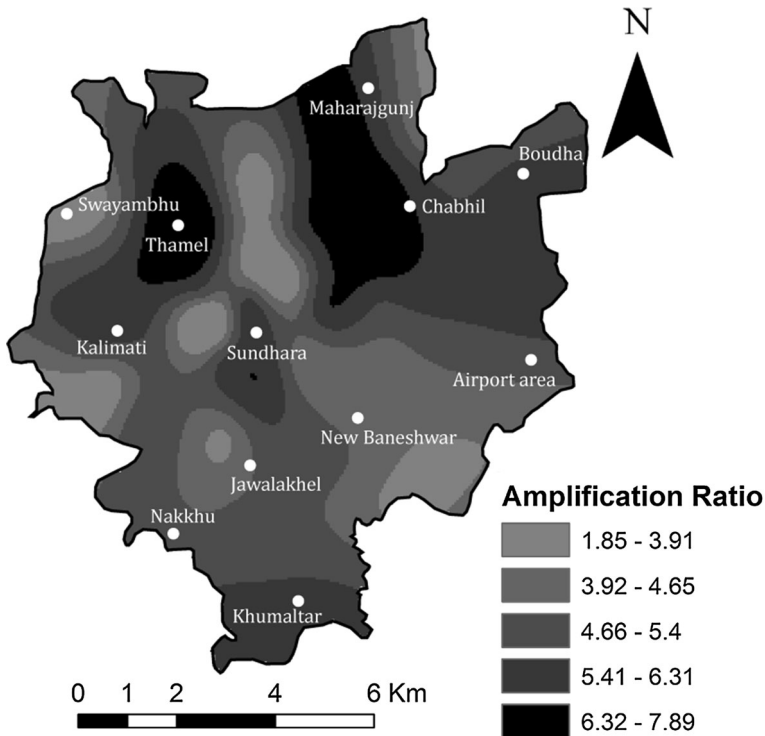


Fig. 11 Amplification ratio distribution in the study area

by low plasticity silty clay and clay. Similarly, the predominant period and peak spectral acceleration are computed as 0.35 s and 1.27 g, respectively, for the Maharajgunj area. In the area, the top layer of the soil has been covered with the filling material and the underlying layers are abundantly composed of silt and sandy facies with low-to-medium plasticity. The lower strata are composed of medium to fine sand with traces of pebbles. East of Maharajgunj, at Dhapasi and Dhumbarahi, the peak spectral acceleration is 1.28 g at the predominant period of 0.27 s. These sites are characterized by medium to coarse sand with pebbles and gravel underlain by the silty sand and fine sand. Similarly, for the Gyaneshwor site, which is mainly characterized by sandy silt underlain by clayey silt of medium plasticity, the peak spectral acceleration is estimated as 1.28 g at predominant period of 0.30 s.

The boreholes from Boudha area have given peak spectral acceleration of 1.28 g at predominant period of 0.27 s. The soil configuration in Boudha area is similar to that of the Thamel, except that traces of pebbles are observed at relatively higher depth. The Chabbil site characterized by silty sand with few layers of clayey silt has shown similar response. The predominant period has been estimated to be 0.30 s with peak spectral acceleration of 1.28 g.

At the central part of the valley, i.e., Sundhara, the value of peak spectral acceleration is relatively higher, i.e., 1.28 g at predominant period of 0.58 s. The geotechnical investigation has shown soil composition to be silty sand underlain by clayey silt for this site. Similarly, for the clay dominant Thapathali area, the spectral acceleration of 1.27 g has

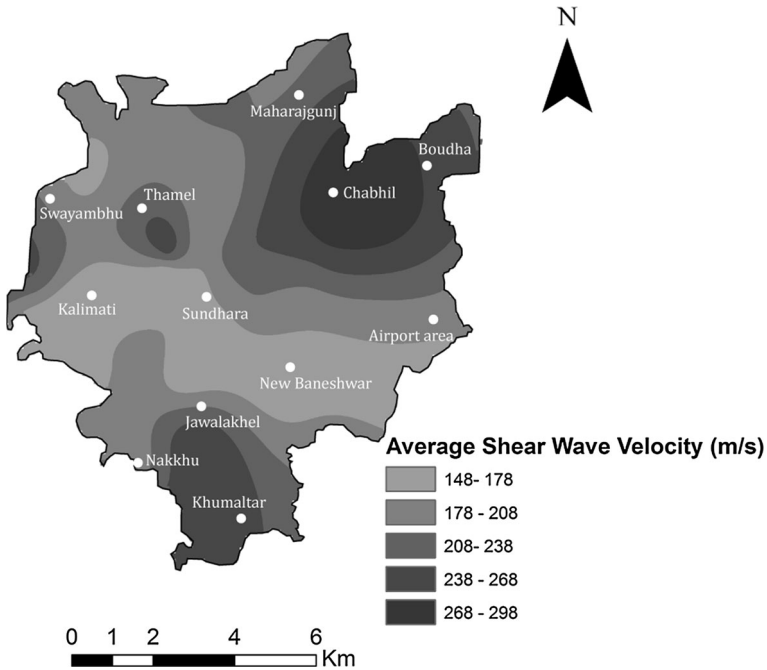


Fig. 12 Average shear wave velocity distribution in the study area

been obtained at 0.46 s. The Jawalakhel area has given peak spectral acceleration of 1.28 g at the predominant period of 0.37 s. Lithologically, area is composed of medium to coarse sand with traces of pebbles, which is underlain by the soft clayey silt. The black clay dominant Kalimati area has given lower peak spectral acceleration at medium predominant period (Fig. 16). The higher predominant period is mainly found to the NE of Thamel and SE of New Baneshwar (Fig. 17).

8 Discussion

8.1 Seismic hazard assessment

There are very limited works on seismic hazard assessment in Kathmandu Valley. JICA (2002) has also conducted seismic hazard, vulnerability and risk assessment and proposed comprehensive disaster management plan. Based on the several scenario earthquakes (e.g., Mid-Nepal earthquake of magnitude 8.0, North Bagmati earthquake of magnitude 6.0, Kathmandu Valley earthquake of magnitude 5.7 and recurrence of 1934 Bihar–Nepal earthquake of magnitude 8.4). Differently, the present study has adopted one-dimensional seismic site effects analysis of upper 30 m of the soft soils deposit using the consistent strong ground motion of Uttarkashi earthquake. The dominance of the building in KMC and LSMC is three to five storied, and thus, based on the current building typology, this study has highlighted the urban seismic hazard for different time periods, e.g., 0.3, 0.4 and

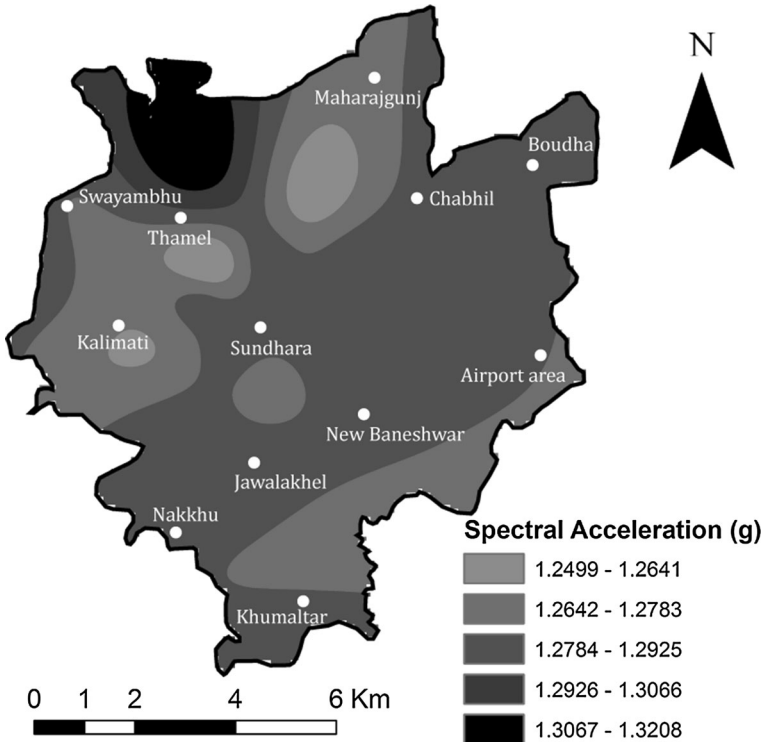


Fig. 13 Spectral acceleration hazard map at 0.3 s

0.5 s. In addition, this study has computed amplification ratio and spectral acceleration for above-mentioned time periods.

In the Kathmandu Valley, the underlying risk of earthquake is mainly inherited on residential building of three to five storied as the buildings lack detail anti-seismic design. However, the probability of ground amplification is high during the earthquake as observed in the past; therefore, their response is significant due to moderate to strong earthquakes like Uttarkashi. Therefore, in this contribution, we show a preliminary evaluation of the site response of upper 30 m soil deposit in KMC and LSMC located in the deep fluvial-lacustrine deposit of the Kathmandu Valley. Although 2D/3D basin geometry has paramount contribution in amplification of incoming wave field causing basin edge effects or valley effects, we employed simple one-dimensional models based on 49 available boreholes.

The study has revealed that the higher shear wave velocity is mainly observed in those sites where the low plasticity silt or even clayey silts were abundant. The impedance contrast contribution to shear wave velocity is more significant than the bulk density as this parameter has no drastic variance within the engineering bedrock level. The maximum peak spectral acceleration is observed in the sites with the silt domination (e.g., Thamel, Boudha, Kalimati, Patan, Sundhara, New Baneshwor, Sinamangal among others) with the peak spectral acceleration value of 1.2826 g governed by high shear wave velocities as well. These areas are important for several aspects; for example, Thamel is tourist center,

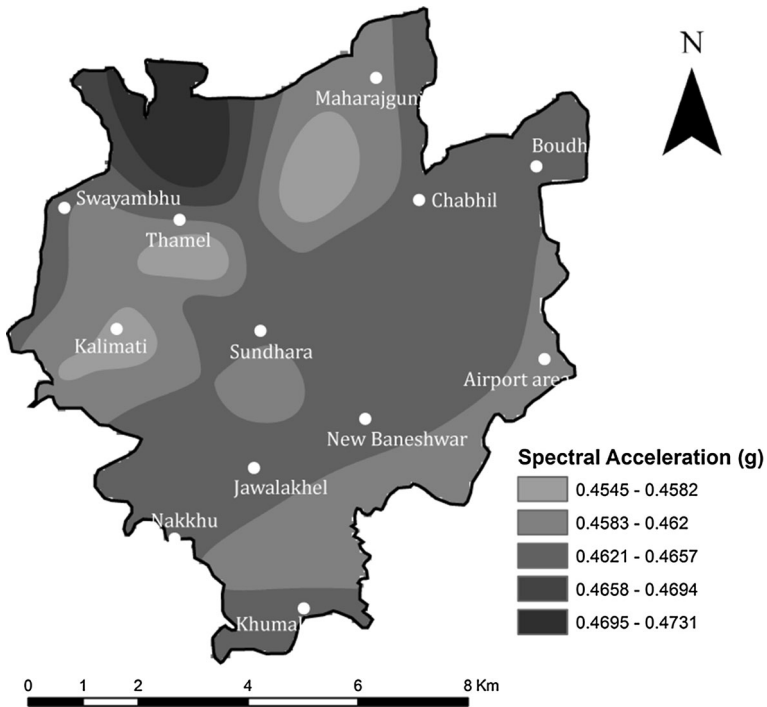


Fig. 14 Spectral acceleration hazard map at 0.4 s

Boudha and Sundhara areas are important cultural sites, and New Baneshwor, Sinamangal and Kalimati are major business centers.

Similarly, amplification of the seismic wave is higher in the clay-dominated sites as compared to sandy areas. The higher values are observed in Thamel, west of Chabhil and Maharajgunj, Sundhara and Khumaltar. In contrast, Dillibazar, Swoyambhu, Balkumari, among others, have been found to be with low amplification ratio as these sites are characterized by alternation of sand and clay up to the engineering bedrock with comparatively moderate values of shear wave velocities. As the sub-layering is directly dependent on the shear wave velocity, the response of the higher shear wave velocity leads to the higher peak spectral acceleration and lower amplification ratio too. The areas (e.g., Thamel, west of Chabhil and Maharajgunj, Sundhara and Khumaltar) with higher amplification ratios are in higher housing risk shown by Bhattarai and Conway (2010). The observed amplification ratios is also consistent with the damage pattern and intensity due to 1934 Bihar–Nepal earthquake. The severe destruction in many sites during 1934 earthquake is also well evidenced by this finding in terms of predominant period and amplification leading to vibration resonance of building with the underlying soil; such destruction was observed in the areas like Maharajgunj, Thamel, Patan, Baneshwor, and in contrast, the areas like Dillibazar, Swoyambhu, among others, experienced less damage. Thus, it is evident that one of the main culprits for 1934 Bihar–Nepal earthquake was seismic wave amplification due to soft clay-dominated soil layers. As the potential sources of earthquake including the central seismic gap are in the range of the modeled Uttarkashi earthquake, such results could better furnish the future seismic site response of soft sediments of

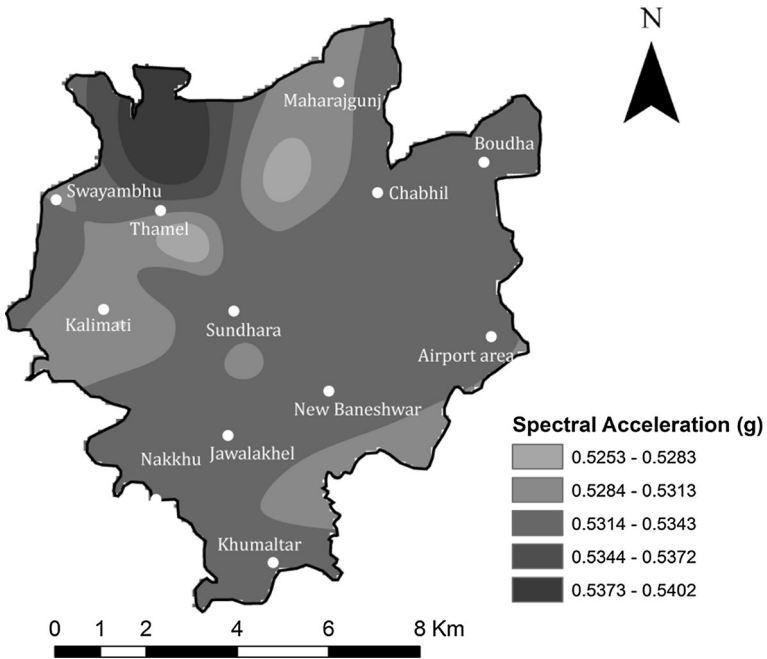


Fig. 15 Spectral acceleration hazard map at 0.5 s

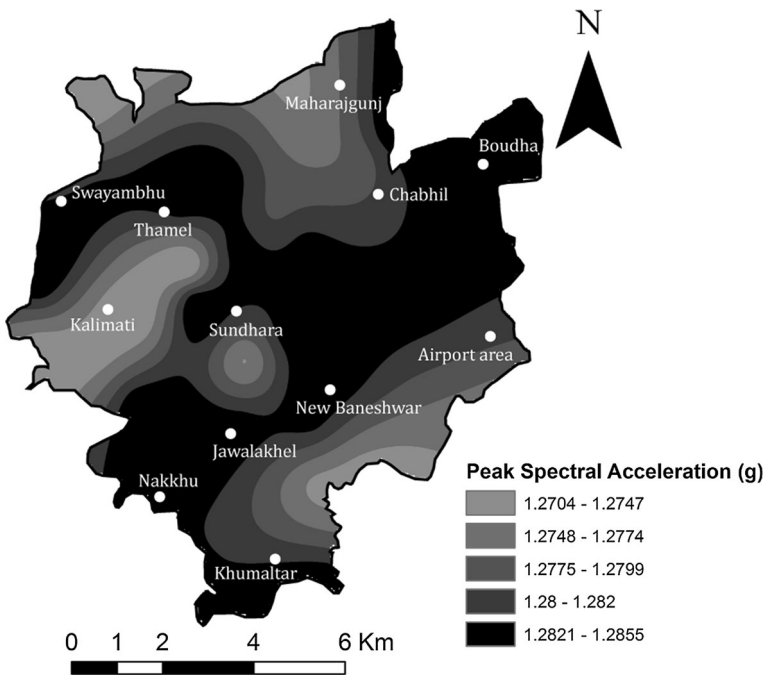


Fig. 16 Peak spectral acceleration hazard map of the study area

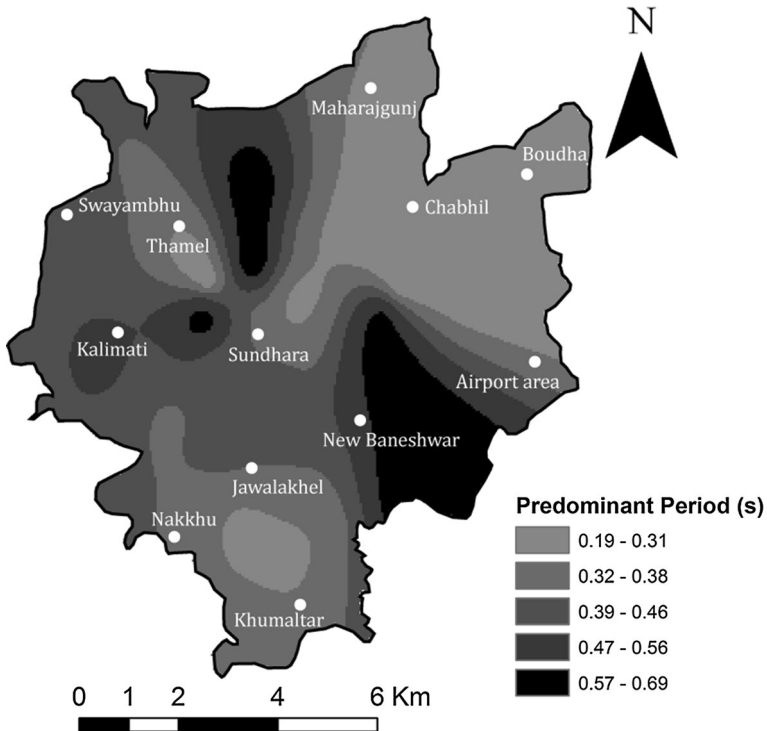


Fig. 17 Predominant period distribution of the study area

Kathmandu Valley. This contribution will be pivotal in terms of site-specific design spectra formulation which is still a hiatus in Nepal Building Code. From the didactic lessons of localized and more scattered damages during 2015 Gorkha earthquake, consideration of seismic site effects and site-specific design spectra are more reinforced. So, the computed parameters and the observed damage patterns have good correlation for soft sediments deposit of Kathmandu Valley and even a good representative model has been presented in this study using a simple one-dimensional equivalent linearization.

8.2 Significance to building damage susceptibility

Many past earthquake events have shown that during strong earthquakes, high seismic intensity is caused mainly due to the soft soil site condition. Almost 98 % of the property damage during 1989 Loma Prieta earthquake was due to ground shaking, thereby causing 70 % of total property damage (Holzer 1994); in this regard, the cities under potential threat of exposure of high energy seismic wave are expected to be analyzed for the case of structural preparedness and hazard assessment. Most of the buildings as per the recent construction trend in Kathmandu Valley are of 3–5 stories, and the possible vibration resonance of structures might further induce the risk level in these cities. Moreover, the past destruction evidence is well correlated with the predominant period of soil in KMC and LSMC; the owner built houses are not incorporated with the earthquake-resistant construction guidelines and practices properly; hence, the vulnerability level is further induced

in these cities. In 2003, building codes were enforced in these cities; however, proper implementation has not been ensured till date so vulnerability level is not remarkably lowered. During the 1934 events, 55,000 buildings were affected in Kathmandu Valley; among these, 12,397 were completely destroyed (Rana 1935), and this damage evidence is also illustrated with the predominant period of soil deposit, as the building construction trend of that period was of 3–5 storied buildings with non-engineered construction practices. Though, the then settlement was not as dense as that of the present-day, future events might further be devastating in Kathmandu Valley, as the construction scenario of 1934 doesn't significantly differ than that of before 2003 and the RC practice of Nepal has not gotten the history of more than 40 years as well. All these evidences along with the inference of Bureau of Crises Prevention and Recovery of the United States Development Program ranking as the 11th most vulnerable country of the world for earthquake disaster; it could be easily contemplated that the Kathmandu Valley construction practices have further accelerated the vulnerability level and future events could generate the massive devastation beyond imagination. Non-engineered structures are ubiquitous in Kathmandu Valley triggering the vulnerability of human settlements and cultural heritage as well, and the accumulated strain level has indicated probability of damaging earthquake which may affect Kathmandu Valley severely. The fundamental period of soil ranges from 0.27 to 0.61 s; hence, possibility of resonance phenomenon during the seismic events is high, so proper implementation of earthquake-resistant construction practices, microzonation, and further studies regarding the seismic site effects are must for earthquake resilient settlements in Kathmandu Valley. The workmanship defects, substandard construction materials, architectural deficiencies, uneven and reclaimed foundation established in slope land are equally exacerbating earthquake risk. Beside these facts, the row housing practices in irregular land plots with unequal story height are the potential sources of pounding effects in the Kathmandu Valley as well. Thus, it is expected that the findings of the present study would greatly contribute to safer construction, earthquake risk management plan and foundation of further research on geotechnical earthquake engineering aspect.

Vibration resonance and seismic demand analysis are key issues in terms of buildings' performance during earthquakes, so the present study mirrors vital insights regarding the seismic demand of buildings in Kathmandu Valley in terms of number of stories, which could be pivotal for building code improvement too. There are number of empirical equations to compare frequency of the buildings with the soil predominant period (e.g., NEHRP 1994; Enomoto et al. 1999). The frequency of the RC buildings in Kathmandu Valley can be calculated and correlated with the soil predominant period as per NEHRP provisions (1994) as per expression 1:

$$T = 0.1 N \quad (1)$$

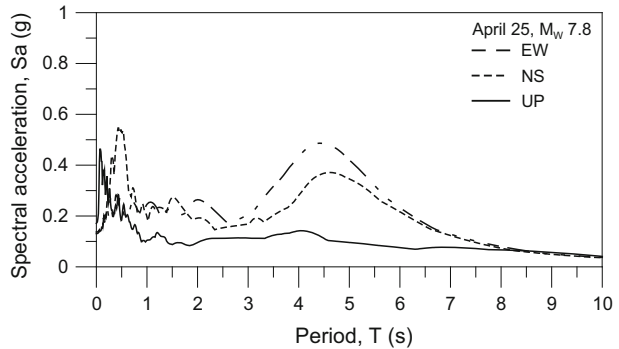
where T suggests natural period of RC building of N stories.

With account of this correlation, RC buildings from 2 to 7 stories are requiring larger seismic demand in terms of design consideration and construction provisions. As most of the RC buildings in the study area are 2–6 stories, careful design and construction is urgently needed for assurance of better performance during future earthquakes. In addition to NEHRP provisions, Enomoto et al. (1999) formulated correlation as in expression 2:

$$T = 0.042 N \quad (2)$$

While considering this expression, the estimated soil predominant period largely correlates the RC buildings ranging from 4.5 to 17 stories. Up to seven stories, there's widespread

Fig. 18 Response spectra (5 % damping) for 2015 Gorkha earthquake computed for Kantipath (central part of the Kathmandu Valley)



presence of residential as well as commercial constructions within Kathmandu Valley. Besides this, the high-rise construction has been reached to 17 stories, and this coincides with the higher seismic demand for middle to high-rise structures of Kathmandu Valley as there's mushrooming trend of construction of such type structures.

During the 2015 Gorkha earthquake, damages in RC buildings was observed in the northern part of Kathmandu Valley as it lies in "red zone"-based PGA and intensity level (Aydan and Ulusay 2015). The PGA at Kantipath (central part of the study area) measured by USGS is about 0.16 g (Kaneko 2015). Although PGA value in the valley is comparatively lower, the non-engineered mud mortar residential houses of 3–6 stories were mostly damaged. The reason behind is probably due to topographic effects because the old cities (e.g., Bhaktapur, Harisiddhi, Bungamati, and Sankhu) are located on the small ridges, which might have amplified the energy of the destructive seismic waves. However, in the core city of Kathmandu, the damage scenario is different. Many of the residential high-rise apartments were severely damaged. The global positioning system (GPS) and strong ground motion data have revealed resonance of the whole basin at 4–5 s period that caused collapse of the tall structures including many of the cultural heritages in the Kathmandu Valley (Fig. 3 of Galetzka et al. 2015). As suggested by NEHRP provisions, there is inherent correlation between the damages in RC buildings. The soil predominant period and building natural periods are also found to be coinciding in the northern part of study area. Like the damages in Gongabu and Sitapaila show good agreement with the significant number of damaged structures. In this regard, vibration resonance surely is a reason triggering extensive damage in northern part of study area. Besides this, the response spectra depicted by USGS show the longer period in 3.5–5.5 s (Fig. 18), and this also justifies the damage concentration in middle to high-rise structures of northern part of Kathmandu Valley. The damage concentration areas in study area are recently incorporated under municipal territory, so prevalent structures do not fulfill the seismic demand in terms of design and construction as well; at the mean time, this study reflects higher seismic demand for middle to high-rise structures. This could be pivotal in terms of performance of buildings during future events in Kathmandu Valley as well.

9 Conclusion

One-dimensional equivalent linear seismic site response analysis for KMC and LSMC has been performed, and the outcomes are presented in the form of amplification ratio, average shear wave velocity spectral acceleration and predominant period. The estimated peak

spectral acceleration varies from 1.2826 to 1.2725 g across Kathmandu Valley; this indicates a very close range distribution of peak spectral acceleration for each study site. The maximum amplification ratio ranges from 1.9 (Sundhara) to 7.8 (Thamel), and entire distribution pattern of amplification is found to be consistent with the damage level observed during 1934 Bihar–Nepal earthquake and the hazard map prepared by JICA (2002). In the same way, the predominant period is found to be varying between 0.27 s (e.g., Boudha, Dhapasi, Dhumbarahi) and 0.61 s (e.g., Balkumari, Lazimpat, Kamaladi). As predominant period and the peak spectral acceleration are more correlated with the damage of structures, in the same way, higher value of peak spectral acceleration has been observed in those areas with the severe damage during the earthquake. It can be inferred that, as observed in the Mexico earthquake, the amplification ratio estimated in the study would be the major culprit for the damages during the impending destructive earthquakes in the Himalayan region. As the present study is limited to 1D assessment, for more precise seismic hazard assessment, valley, topographic and basin effects, as seen in 2015 Gorkha earthquake, should be studied adopting 2D simulation for better assessment of earthquake risk in the Kathmandu Valley.

Acknowledgments The authors express sincere thanks to Er. Raghu N Prajapati, Assistant Professor, Nepal Engineering College, Pokhara University, for his help in drafting map in ArcGIS environment. Mr. Murali Narayan Deo, Multi Lab Pvt. Ltd, is thanked for providing us extensive borehole logs of Kathmandu and Lalitpur cities.

Compliance with ethical standards

Conflict of interest The authors declare that they have no conflict of interest.

References

- Aki K (1993) Local site effects on weak and strong ground motion. *Tectonophysics* 218:93–111
- Aki K, Larner KL (1970) Surface motion of a layered medium having an irregular interface due to incident plane SH waves. *J Geophys Res* 75:933–954
- Avouac JP, Meng L, Wei S, Wang T, Ampuer JP (2015) Lower edge of locked Main Himalayan Thrust unzipped by the 2015 Gorkha earthquake. *Nat Geosci* 8:708–711. doi:10.1038/ngeo2518
- Aydan Ö, Ulusay R (2015) A quick report on the 2015 Gorkha (Nepal) earthquake and its geo-engineering aspects. http://www.iaeg.info/wpcontent/uploads/QuickRepot_2015NepalEarthquake_Aydan_Ulusay_IAEG.pdf
- Baranowski J, Armbruster J, Seeber L, Molnar P (1984) Focal depths and fault plane solutions of earthquakes and active tectonics of the Himalaya. *J Asian Earth Sci* 29:473–489
- Bardet JP, Ichii K, Lin CH (2000) EERA: a computer program for equivalent linear earthquake site response analyses of layered soil deposits. Department of Civil Engineering, University of Southern California
- Bhattarai K, Conway D (2010) Urban vulnerabilities in the Kathmandu Valley, Nepal: visualizations of human/hazard interactions. *J Geogr Inf Syst* 2:63–84
- Bilham R (1995) Location and magnitude of the 1833 Nepal earthquake and its relations to the rupture zones of contiguous great Himalayan earthquakes. *Curr Sci* 69(2):101–128
- Bilham R, Ambraseys N (2004) Apparent Himalayan slip deficit from the summation of seismic moments for Himalayan earthquakes, 1500–2000. *Curr Sci* 88(10):1658–1663
- Bilham R, Bodin P, Jackson M (1995) Entertaining a great earthquake in western Nepal: historic inactivity and geodetic tests for present state of strain. *J Nepal Geol Soc* 11(1):73–78
- Bilham R, Gaur VK, Molnar P (2001) Himalayan seismic risk. *Science* 293:1442–1444
- CBS (Central Bureau of Statistics) (2011) National population and housing census 2011 (national report), vol 01. Government of Nepal, NPHC 2011
- Celebi M, Prince J, Dietel C, Onate M, Chavez G (1987) The culprit in Mexico City—amplification of motions. *Earthq Spectra* 3:315–328

- Chamlagain D, Gautam D (2014) Seismic hazard in the Himalayan intermontane basins: an example from Kathmandu valley, Nepal. In: Shaw R, Nibanupudi HK (eds) Mountain hazards and disaster risk reduction. Springer, Tokyo, pp 73–103
- Chamlagain D, Hayashi D (2007) Neotectonic fault analysis by 2D finite element modeling for studying the Himalayan fold and thrust belt in Nepal. *J Asian Earth Sci* 29(2007):473–489
- Chamlagain D, Lanzo G, Pagliaroli A, Scasserra G (2013) Numerical simulation of site effects in the upper Aterno valley array during the aftershock sequence of the 2009 L'Aquila earthquake. *Riv Ital Geotech* 4(2013):8–23
- Chen Z, Burchfiel BC, Liu Y, King RW, Royden LH, Tang Wang E, Zhao J, Zhang X (2000) Global Positioning Systems measurements from eastern Tibet and their implications for India/Eurasia inter-continental deformation. *J Geophys Res* 105(B7):16215–16227
- Chitrakar GR, Pandey MR (1986) Historical earthquakes of Nepal. *Bull Geol Soc Nepal* 4:7–8
- Dill HG, Kharel BD, Singh VK, Piya A, Busch K, Geyh M (2001) Sedimentology and paleogeographic evolution in the intermontane Kathmandu basin, Nepal, during Pliocene and Quaternary. Implication for formation of deposit of economic interest. *J Asian Earth Sci* 19:777–804
- Dill HG, Khadka DR, Khanal R, Dohrmann R, Melcher F, Busch K (2003) Infilling of the Younger Kathmandu-Banepa intermontane lake basin during the Late Quaternary (Lesser Himalaya, Nepal): a sedimentological study. *J Quat Sci* 18(1):41–60
- Enomoto T, Navarro M, Sánchez F, Vidal F, Seo K, Luzón F et al (1999) Evaluación del comportamiento de los edificios en Almería mediante el análisis del ruido ambiental, 1a Asamblea Hispano-Lusa. Aguadulce, Almería, Spain
- Galetzka J et al (2015) Slip pulse and resonance of Kathmandu basin during the Mw 2015 Gorkha earthquake, Nepal imaged with geodesy. *Science* 349(6252):1091–1095. doi:10.1126/science.aac6383
- Gupta SP (1988) Eastern Nepal earthquake 21 August 1988, damage and recommendations for repairs and reconstruction. Asian Disaster Preparedness Center, Asian Institute of Technology, Bangkok
- Holt WE, Chamot-Rooke N, Le Pichon X, Haines AJ, Shen-Tu B, Ren J (2000) Velocity field in Asia inferred from Quaternary fault slip rates and global positioning system observations. *J Geophys Res* 105(B8):19185–19209
- Holzer TL, Tinsley JC, Benette MJ, Mueller CS (1994) Observed and predicted ground deformation-Miller Farm lateral spread, Watsonville California. In: Proceeding of the 6th US Japan Workshop on Earthquake Resistant Design of Lifelines facilities and countermeasures for Soil Liquefaction, pp 79–98
- JICA (Japan International Cooperation Agency) (2002) The study on earthquake disaster mitigation in the Kathmandu Valley, Kingdom of Nepal, vol I. Japan International Cooperation Agency (JICA) and Ministry of Home Affairs, His Majesty's Government of Nepal, p 110
- Jouanne F, Mugnier JL, Gamond JF, Le Fort P, Pandey MR, Bollinger L, Flouzat M, Avouac JP (2004) Current shortening across the Himalayas of Nepal. *Geophys J Int* 157:1–14
- Kaneko F (2015) Flash report on damages by the 2015 Gorkha earthquake. OYO International Corporation. http://www.oyointer.com/english/KTM_EQ/KTM_EQ_EN_REP.pdf
- Katel TP, Upreti BN, Pokharel GS (1996) Engineering properties of fine grained soils of Kathmandu Valley, Nepal. *J Nepal Geol Soc* 13:121–138
- Lanzo G, Silvestri F, Costanzo A, d'Onofrio A, Martelli L, Pagliaroli A, Sica S, Simonelli A (2011) Site response studies and seismic microzoning in the Middle Aterno valley (L'Aquila, Central Italy). *Bull Earthq Eng* 9(5):1417–1442
- Molnar P (1984) Structure and tectonics of the Himalaya: constraints and implications of geophysical data. *Ann Rev Earth Planet Sci* 12:489–518
- Molnar P, Lyon-Caen H (1989) Fault plane solutions of earthquakes and active tectonics of the Tibetan Plateau and its margins. *Geophys J Int* 99:123–153
- Moribayashi S, Maruo Y (1980) Basement topography of the Kathmandu Valley, Nepal—an application of gravitational method to the survey of a tectonic basin in the Himalayas. *J Jpn Soc Eng Geol* 21(2):30–37
- NEHRP Recommended Provisions for New Buildings (1994) Building Seismic Safety Council, Washington
- Ni J, Barazangi M (1984) Seismotectonics of the Himalayan collision zone: Geometry of the underthrusting Indian plate beneath the Himalaya. *J Geophys Res* 89:1147–1163
- Pandey MR, Molnar P (1988) Distribution of intensity of the Bihar–Nepal earthquake 15 January 1934 and bounds on the extent of rupture. *J Nepal Geol Soc* 5(1):22–44
- Pandey MR, Tandukar RP, Avouac JP, Lave J, Massot JP (1995) Interseismic strain accumulation in the Himalayan crustal ramp (Nepal). *Geophys Res Lett* 22:751–754
- Pandey MR, Tandukar RP, Avouac JP, Vergne J, Heirittier T (1999) Seismotectonics of the Nepal Himalaya from a local seismic network. *J Asian Earth Sci* 17:703–712

- Patriat P, Achache J (1984) Indian-Eurasian collision chronology has implications for crustal shortening and driving mechanism of plates. *Nature* 311:615–621
- Paul J, Burgmann R, Gaur VK, Bilham R, Larson K, Ananda MB, Jade S, Mukul M, Anupama TS, Satyal G, Kumar D (2001) The motion and active deformation of India. *Geophys Res Lett* 28(4):647–650
- Psarropoulos PN, Gazetas G, Tazoh T (1999) Seismic response analysis of alluvial valley at bridge site. In: 2nd international conference in earthquake geotechnical engineering, Lisbon, pp 41–46
- Psarropoulos PN, Tazoh T, Gazetas G, Apostolou M (2007) Linear and nonlinear valley amplification effects on seismic ground motion. *Soil Found* 47(5):857–871
- Rana BSJB (1935) The great earthquake of Nepal ('Nepalko Mahavukampa', in Nepali). Jorganesh Press, Kathmandu
- Rowley DB (1996) Age of initiation of collision between India and Asia: a review of stratigraphic data. *Earth Planet Sci Lett* 145:1–13
- Sakai H (2001a) The Kathmandu Basin: an archive of Himalayan uplift and past monsoon climate. *J Nepal Geol Soc* 25(special issue):1–8
- Sakai H (2001b) Core drilling of the basin-fill sediments in the Kathmandu Valley for paleoclimatic study: preliminary results. *J Nepal Geol Soc* 25(special issue):9–18
- Sakai H (2001c) Stratigraphic division sedimentary facies of the Kathmandu basin group, Central Nepal. *J Nepal Geol Soc* 25(special issue):19–32
- Seeber L, Armbruster J (1981) Great detachment earthquakes along the Himalayan arc and the long term forecasts. In: Simpson EW, Richards PG (eds) *Earthquake prediction: an international review*, Maurice Ewing series 4. American Geophysical Union, Washington, pp 259–277
- Seeber L, Armbruster J, Quittmeyer RC (1981) Seismicity and continental subduction in the Himalayan arc, in Zagros, Hindu-Kush-Himalaya, geodynamic evolution. *Geodyn Ser* 3:215–242
- Sella GF, Dixon TH, Mao A (2002) REVEL: a model for recent plate velocities from space geodesy. *J Geophys Res: Solid Earth* (1978–2012) 107(B4):ETG-11
- Semblat JF, Kham M, Bard PY, Gueguen P (2004) Could 'site-city interaction' modify site effects in urban areas? In: 13th world conference on earthquake engineering, Vancouver, paper no. 1978
- Stocklin J, Bhattarai KD (1977) *Geology of Kathmandu area and central Mahabharat range, Nepal Himalaya*. HMG/UNDP Mineral Exploration Project, Kathmandu
- Upreti BN (1999) An overview of the stratigraphy tectonics of the Nepal Himalaya. *J Asian Earth Sci* 17(1999):577–606
- Upreti BN, Le Fort P (1999) Lesser Himalayan crystalline nappes of Nepal: problem of their origin. In: Macfarlane A, Quade J, Sorkhabi (eds) *Geological Society of America special paper 328*, pp 225–238
- USGS (United States Geological Survey), 2011. <http://www.usgs.gov/>
- Vucetic M, Dobry RJ (1991) Effect of soil plasticity on cyclic response. *J Geotech Eng ASCE* 117:89–117
- Wang Q, Zhang P, Freymueller J, Bilham R, Larson K, Lai X, You X, Niu Z, Wu J, Li Y, Liu J, Yang Z, Chen Q (2001) Present day crustal deformation China constrained by global positioning system measurements. *Science* 294:574–577
- Yoshida M, Igarashi Y (1984) Neogene to Quaternary lacustrine sediments in the Kathmandu valley, Nepal. *J Nepal Geol Soc* 4:73–100
- Zhang P, Shen Z, Wang M, Gan W, Burgmann R, Molnar P, Wang Q, Niu Z, Sun J, Wu J, Hanrong S, Xinzhao Y (2004) Continuous deformation of the Tibetan Plateau from global positioning system data. *Geology* 32(9):809–812